Nanopatterning using a simple bilayer lift-off process by transfer printing based on poly(dimethylsiloxane) templates

Dingjie Zheng, Dong Dong, Aixia Sang, Zhengqiaoruo Zhu, Min Zhu, Xudi Wang

School of Mechanical and Automotive Engineering, Hefei University of Technology, Hefei 230009, People's Republic of China
E-mail: wxudi@hfut.edu.cn

Published in Micro & Nano Letters; Received on 17th May 2015; Revised on 10th September 2015; Accepted on 14th September 2015

An efficient and versatile method for fabricating nanopatterns by a lift-off procedure is presented. The method involves an inked technique based on the poly(dimethylsiloxane) (PDMS) mould to fabricate a nanopatterned UV-curable resist as the top-layer and poly(methyl methacrylate) (PMMA) as the underlayer. The minimal residues are left on the PMMA because PDMS absorbs the organic molecules of UV-curable resist after the transferred step. High O_2 reactive ion etching selectivity of the top-layer to the underlayer is necessary to create the undercut pattern profile that is essential for the stable lift-off process. The UV-curable resist shows high etch resistance to O_2 plasma and PMMA serves as an underlying resin to create an undercut profile which is essential for the lift-off process. The etch rates of the PMMA film and UV-curable resist by O_2 plasma were examined as a function of bias voltage under various oxygen conditions during the etching process. To reveal the mechanism of etch resistance, the chemical composition of UV-curable resist was analysed before and after the O_2 plasma etching process by using X-ray photoelectron spectroscopy. As a result, the periodical patterns were fabricated using this bilayer lift-off process, which shows great potential in the fabrication of micro/nanodevices and in their applications.

1. Introduction: The lift-off process has been demonstrated to be a very efficient method for fabricating nanosized metal patterns. A lift-off typically involves using lithography to fabricate a pattern in photoresist and metal deposition. To obtain well-fabricated patterns following stripping, an undercut pattern profile is essential for the stable lift-off process [1]. So far, pattern transfer using a single layer of resist [2], a bilayer resist [3] and a trilayer structure [4] has been reported. Although the process of the single-layer technique is simple, its reliability is doubtful because it is difficult to form the undercut pattern profile for lift-off and it needs the reactive ion etching (RIE) process to remove the residual resist. The reported trilayer techniques such as Su-8/SiO_2/poly(methyl methacrylate) (PMMA) [5] do have improved reliability and critical dimension controllability, but they demand an oxide deposition step, which greatly affects the efficiency of the process. For the lift-off process using bilayer procedures, the underlayer is typically formed by the polymeric material beneath the patterned top-layer formed by the photoresist prior to material deposition. To create the undercut pattern profile, the O_2 plasma etch resistance of the underlayer material must be lower than that of the transferred resist pattern.

The lift-off procedures have been typically used for forming well-resolved structures by nanoimprint, where a patterned template is imprinted into the imprint resin to fabricate the patterned layer. There still are some challenges to face for lift-off using bilayer nanoimprint lithography (NIL). The traditional imprint resins have poor etch resistance to most plasmas, thus there is a limitation to them as an etch mask. Near-zero residues are rather difficult to achieve unless a higher pressing force is applied to the imprint process. To settle such problems of large-area low-cost patterning, a straightforward lift-off procedure, which involves its innovation of using nanopattern manufacture in a bilayer structure by transfer printing based on the poly(dimethylsiloxane) (PDMS) mould, has been demonstrated in this Letter. We can achieve minimal residues left after the transfer printing step because the elastic substrate with multifunctional low-viscous photocurable resist would be absorbed by the intrinsic high permeability of PDMS. An UV-curable organo-silicon resist with high O_2 etch resistance and capability of diffusing into the PDMS network was used for transfer printing assisted by UV-curing [6]. The high-fidelity lift-off process was demonstrated that it is in need of high O_2 plasma etch selectivity of the imprinted resist pattern to the underlayer. Owing to the simplicity of this novel method, the manufacture of large-area nanostructures which are fabricated by firm or flexible materials is easily scaled, and may enable laboratories without high-end facilities to get involved in the manufacturing of micro/nanodevices and in their applications.

2. Experiment: The work started with the duplication of PDMS stamping from a quartz mould. The laser interference lithography (Kr+laser, $k = 423.1$ nm) had made patterns on the mould with a period of 1000 nm on a photoresist-coated quartz substrate. To etch into the quartz substrate, the mask was fabricated by the photoresist line pattern in following reactive ion beam etching. By casting PDMS (Sylgard 184, Dow Corning) precursors (with 10 wt% curing agent) against the masters, the PDMS mould was prepared, resulting in a complementary relief structure followed by curing at 150°C for 15 min. Finally, the PDMS mould could be peeled off from the silicon template along the direction of lines [7]. Fig. 1 shows the overall process flow for the fabrication of the metal pattern in this Letter. A self-made liquid UV-curable resist is used in this process. The resist is made of low viscous, photocurable liquid materials based on multifunctional acrylate groups, and a polysiloxane derivative which could increase the O_2 etch resistance of the resist. The resist was spin coated on the silicon wafer by 2000 rpm for 60 s to obtain a 200 nm thick layer. The PDMS mould with nanosized patterns was then placed on the photoresist film and kept in uniform contact for the diffusion of photocurable molecules into the PDMS network through the contact surface between the PDMS surface and the resist film. The UV resist was filled into the cavities of the PDMS by capillary action spontaneously and rapidly. The PDMS stamp was peeled off from the silicon substrate after an equilibration time of absorption and resist filling about 1 min. A 200 nm-thick PMMA layer was spin coated on the silicon substrate and pretreated at 180°C on a hot plate for 1 h. The PMMA layer should be treated by O_2 plasma, which could help to transfer the photoresist pattern successfully onto the PMMA layer. The PDMS stamp with the UV-curable resist was cautiously placed onto the PMMA layer. A large area of patterned resist can be obtained on the underlayer by soft and

© The Institution of Engineering and Technology 2015

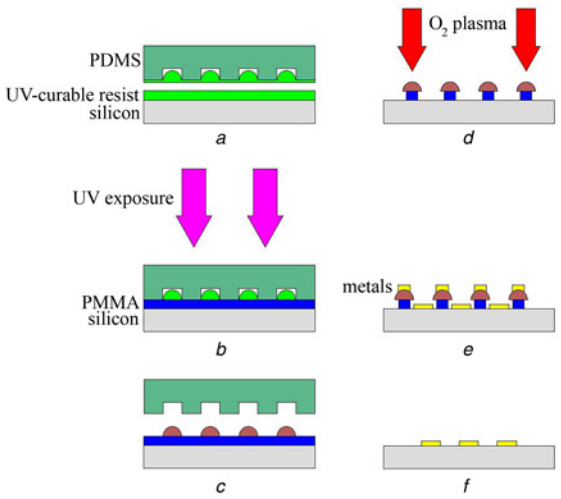

Fig. 1 *Overall process flow for the fabrication of the metal pattern*
a UV resist was filled into the PDMS's cavities
b PDMS stamp absorbed with photocurable resist was carefully placed onto the silicon substrate spin-coated with PMMA layer and the sandwich was exposed to UV light
c After separation, the cross-linked photocurable resist on the PDMS mould was transferred onto the PMMA
d PMMA underlayer was etched by O_2 RIE to create the undercut pattern profile
e Metal was deposited
f Lift-off

flexible advantages of the PDMS without external force. Flood UV exposure (wavelength: 365 nm) through the sandwich was carried onto cross link the whole UV resist lamination for 10 min. For preventing the oxygen diffusing into the PDMS, the UV-curing process was executed in a nitrogen atmosphere. After separation, the patterned top-layer duplicated from the PDMS mould was transferred onto the PMMA underlayer. Then the PMMA underlayer was etched by O_2 RIE to create the undercut pattern profile for the high-fidelity lift-off process and the UV-curable resist pattern was used as an etch mask. Subsequently, the Au film was coated by e-beam evaporation and the lift-off process was carried out by dissolving the underlayer in acetone. The etch rates of PMMA and UV-curable resist were calculated from the etched depth and the etching time, with the etched depth measured by the Tencor Alpha Step-500 stylus profilometer. In addition, the pattern profiles were examined by JSM-6700F scanning electron microscope (SEM). The surface chemical compositions of the UV resist before and after O_2 plasma etching were investigated by ESCALAB250 X-ray photoelectron spectroscopy (XPS).

3. Results and discussion: Fig. 2 shows the SEM images of patterns of the bilayer resist structure before and after the O_2 plasma etching process (Figs. 2*a* and *b*). It can be seen that the grating structures of UV-curable resist have been transferred onto the underlayer successfully and near-zero residues have been observed at the bottom of transfer-printed gratings. The result indicates that the photocurable molecules diffusing into the PDMS mould could be cured during UV exposure, which is difficult to be left on the surface of the PMMA layer. However, the UV-curable resist filling into the cavity of the PDMS mould may react with the –OH group of the PMMA surface to form covalent bonding before and during the curing process.

High O_2 RIE selectivity of the UV-curable resist pattern to the underlayer, which is necessary to create an undercut pattern profile, is essential for the lift-off process. The etch rates of PMMA and UV-curable resist by O_2 plasma were examined as a function of bias voltage. In the experiments, the flow rate of O_2 was fixed at 30 sccm and the chamber pressure was maintained at

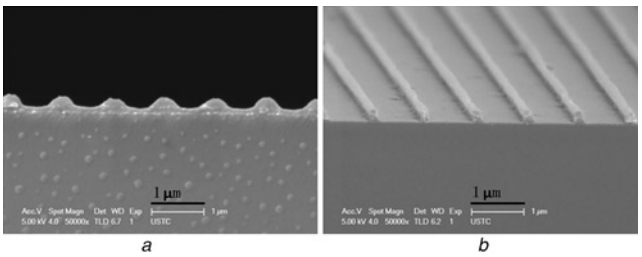

Fig. 2 *SEM images of the bilayer structure*
a Cross-sectional SEM image before etching by O_2 plasma
b Cross-sectional SEM image after etching by O_2 plasma

30 mTorr. The etch rates of UV-curable resist and PMMA have been plotted in Fig. 3 as a function of square root of bias voltage. The results are in good agreement with Steinbruche's [8] theory which is expressed by the following equation

$$ER(E_i) = A(E_i^{1/2} - E_{\text{th}}^{1/2}) \tag{1}$$

where A (slope) and E_{th} (reactive sputter threshold bias voltage) were constants depending on the ion–substrate combination and E_i is directly proportional to the bias voltage generated by the RF power source on the cathode. In the experiments, the RF power varied from 15 to 40 W.

By a least-squares fit of (1), Fig. 3 shows that every group of corresponding data has been demonstrating a linear dependency between etch rates and $V^{1/2}$. The constants in (1), derived from the fitting, are listed in Table 1. As a sign of the quality of curve fitting, Table 1 shows the value of adj·r^2 (square of the correlation coefficient) for each fitted plot. The bias voltage's threshold value of the PMMA is 62.7 V; however, the bias voltage's threshold value of the UV-curable resist cannot be obtained from Table 1. It is implied the UV-curable resist has much higher threshold of bias voltage than that of PMMA. Fig. 3 shows that the ion energy and active radicals increase with bias voltage increasing,

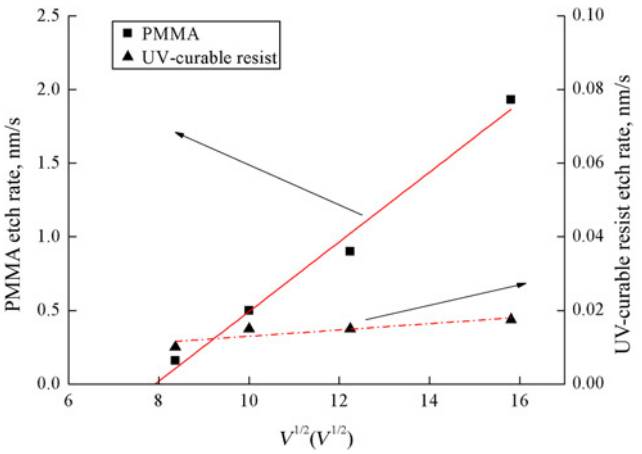

Fig. 3 *Etch rate as a function of $V^{1/2}$ in various O_2 plasma with a gas flow rate of 30 sccm and an etch time of 10 min*

Table 1 Experimentally derived constants in the equation $ER(E_i) = A(E_i^{1/2} - E_{\text{th}}^{1/2})$ for RIE of PMMA and UV-curable resist

Substrate	Gas	A	V_{th}	adj·r^2
PMMA	O_2	0.23657	62.7	0.998
UV-curable resist	O_2	0.00443	$+\infty$	0.969

© The Institution of Engineering and Technology 2015

doi: 10.1049/mnl.2015.0207

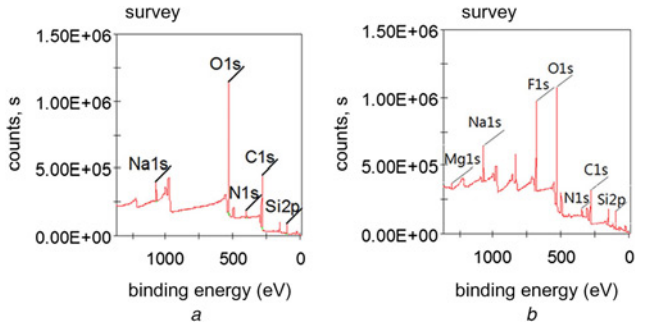

Fig. 4 *XPS spectra of the UV-curable resist*
a Before oxygen plasma etching
b After oxygen plasma etching

thus the physical and chemical effects of the RIE process have increased simultaneously. The results revealed that PMMA not only has a higher etch rate than UV-curable resist at the same experimental conditions, but also the O_2 RIE sensitivity of PMMA, which is expressed by the constant A in (1), is rather higher than the UV-curable resist. It is proved that the bilayer structure using UV-curable resist as the top layer and PMMA as underlayer is well applicable for the lift-off process.

To reveal the mechanism of etch resistance of UV-curable resist, the chemical composition of UV-curable resist was analysed before and after the O_2 plasma etching process by using XPS. The chemical make-up of the top-layer film is analysed by XPS up to a depth of 5–8 nm [9]. The XPS spectra of the UV-curable resist before oxygen plasma etching (Fig. 4*a*) and after the O_2 plasma etching (Fig. 4*b*) is shown in Fig. 4. Fig. 4*a* shows that the UV-curable resist is mainly composed of C, N, O, Si. The spectra were deconvoluted into different peaks for different chemical groups. Fig. 4*a* was deconvoluted into different C1S peaks for different chemical groups, which were assigned to C–H (C1:284.5 eV) [10], C–O (C2:285.5 eV) [11], C=O (C3:288.5 eV) and a weak peak (just below 292.0 eV) stemming from a π–π* shake-up process. In the Si2p band, the major peaks were Si–O (Si1:102.5 eV), Si–C (Si2:101.3 eV) [12] and SiO_2 (Si3:103.0 eV). Comparing Figs. 4*a* and *b*, the XPS peak of SiO_2 sharply increased and the Si–O related peak sharply decreased, the Si–C related peak also decreased. After etching by O_2 plasma, the quantity of C sharply decreased due to the decrease in the quantity of the C of the C–H. On the other hand, we can see the quantity of C was decreased while the Si and O were increased after the O_2 plasma etching process.

Table 2 shows the quantitative change content of, from Figs. 4*a* to *b*, C, O, Si. The O/C and Si/C of UV-curable resist were both increased after O_2 plasma treatment. The surface of the UV-curable resist, which contains Si, is generally oxidised and formed the thin layer of SiO_2 by being exposed to O_2 plasma, thus it has a high resistance to O_2 RIE because the oxidised surface acts as the masking layer to O_2 plasma.

The consequence of this lift-off technique has demonstrated that the periodic structures could be well fabricated and observed. The SEM images show patterns of the dots and the gratings achieved using the method in Fig. 5. It is obvious that the undercut structures have been formed in the bottom layer (Figs. 5*a* and *c*). The Au patterns with a diameter of 480 nm and 90 nm thicknesses were

Table 2 Content variations in C, O and Si before and after O_2 plasma treatment of the UV-curable resist

Fig	C, %	O, %	Si, %	O/C	Si/C
a	48.56	37.53	8.16	0.773	0.168
b	34.86	46.26	18.89	1.327	0.542

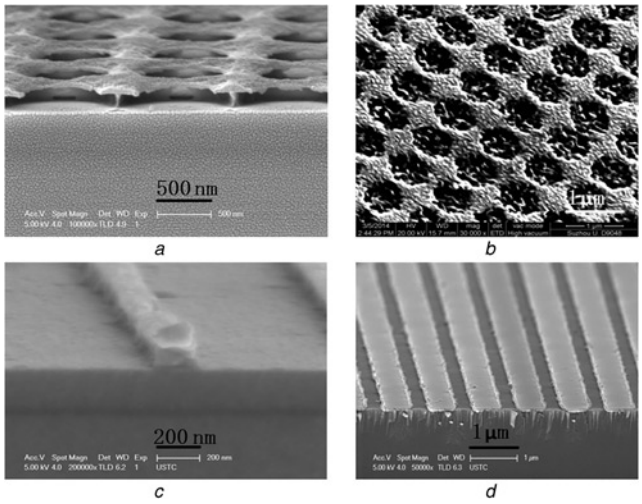

Fig. 5 *SEM images of nanopatterns*
a and *c* SEM images after O_2 RIE
b Top-down SEM images of the nanodots
d Cross-sectional SEM images of the gratings

successfully transferred onto the silicon wafer substrate. A droplet of the etchant mixture, consisting of HF, H_2O_2 and H_2O is placed onto the sample and the etching takes place. For fabricating structured dots in silicon, the Au mask moves with the etching front. The silicon nanodots were finally fabricated by metal-assisted chemical etching (Fig. 5*b*). In Fig. 5*d*, the gratings of Au with a linewidth of 600 nm and the thicknesses of 20 nm were obtained after the lift-off process. As a result, this technique possesses several advantages. First, a large area of pattern which is conformably over a range of substrates can be formed by the transfer printing process based on the flexibility of the PDMS mould. Second, because of the high etch resistance of the UV-curable resist, the undercut pattern profile is easy to create and the bilayer process is reliable. Finally, the PDMS mould could absorb the photocurable molecules, which is the key issue to achieve minimal residues.

4. Conclusion: A lift-off procedure involving an inked process of UV-curable resist based on PDMS moulds has been demonstrated. We use the PDMS mould with the capability of absorbing the photocurable molecules to obtain the transferred top patterns with the minimal residual layer. The organosilicon-based UV resin showed high etch resistance to O_2 plasma, and the undercut pattern profile of the PMMA underlayer for the lift-off process was formed by the O_2 plasma etching process. The size and shape of the transferred resist were hardly affected during the oxygen plasma etching process. Consequently, the reliable and high-fidelity metal periodic structures were fabricated by the lift-off process with a patterned UV-curable resist as the top resin and the PMMA as the underlying resin. The proposed bilayer structure which is an efficient and relatively simply technique for forming nanopatterns has been demonstrated, thus a widely varied fabrication process where nanostructure surfaces are needed can be efficiently fabricated using this structure. The simplicity and high efficiency of this technique would promote its applications in large-area nanostructure fabrication process.

5. Acknowledgments: This work was supported by the National Natural Science Foundation of China (grant no. 61574053).

6 References

[1] Chen Y., Peng K., Cui Z.: 'A lift-off process for high resolution patterns using PMMA/LOR resist stack', *Microeleron., Eng.*, 2004, **73–74**, pp. 278–281

© The Institution of Engineering and Technology 2015

[2] Chou S.Y., Krauss P.R., Renstrom P.J.: 'Imprint of sub-25 nm vias and trenches in polymers', *Appl. Phys. Lett.*, 1995, **67**, (10–11), pp. 1537–1544
[3] Belotti M., Torres J., Roy E.: 'Fabrication of SOI photonic crystal slabs by soft UV-nanoimprint lithography', *Microeleron., Eng.*, 2006, **83**, (4–9), pp. 1773–1777
[4] Tallal J., Berton K., Gordon M.: '4 Inch lift-off process by trilayer nanoimprint lithography', *J. Vac. Sci. Technol. B*, 2005, **23**, (6), pp. 2914–2919
[5] Wan J., Shu Z., Deng S.R., Xie S.Q.: 'Duplication of nanoimprint templates by a novel SU-8/SiO_2/PMMA trilayer technique', *J. Vac. Sci. Technol. B*, 2009, **27**, (1), pp. 19–22
[6] Li Z.W., Gu Y.N., Wang L.: 'Hybrid nanoimprint-soft lithography with sub-15 nm resolution', *Nano Lett.*, 2009, **9**, (6), pp. 2306–2310
[7] Cui Z.: 'Nanofabrication technologies and application', Beijing, PR China, 2009, pp. 252–253; 262–263
[8] Steinbruchel C.: 'Universal energy dependence of physical and ion-enhanced chemical etch yields at low ion energy', *Appl. Phys. Lett.*, 1989, **55**, (19), pp. 1960–1962
[9] Kole A., Chaudhuri P.: 'Growth of silicon quantum dots by oxidation of the silicon nanocrystals embedded within silicon carbide matrix', *AIP Advances*, 2014, **4**, (10), p. 107106
[10] El Khakani M.A., Chaker M., Jean J., Boily S.: 'Effect of rapid thermal annealing on both the stress and the bonding states of a −SiC:H film', *Appl. Phys. Lett.*, 1993, **74**, (4), pp. 2834–2840
[11] Choi W.K., Loo F.L., Ling C.H.: 'Structural and electrical studies of radio frequency sputtered hydrogenated amorphous silicon carbide films', *Appl. Phys. Lett.*, 1995, **78**, (12), pp. 7289–7294
[12] Gat E., El Khakani M.A., Chaker M.: 'A study of the effect of composition on the microstructural evolution of a$-Si_x-C_{1-x}$:H PECVD film:IR absorption and XPS characterizations', *Mater. Res*, 1992, **7**, (9), pp. 248–2787

© The Institution of Engineering and Technology 2015

doi: 10.1049/mnl.2015.0207